

LETTER • OPEN ACCESS

Extreme event impacts on CO₂ fluxes across a range of high latitude, shrub-dominated ecosystems

To cite this article: Rachael Treharne *et al* 2020 *Environ. Res. Lett.* **15** 104084

View the [article online](#) for updates and enhancements.



OPEN ACCESS

RECEIVED
9 May 2020**REVISED**
29 July 2020**ACCEPTED FOR PUBLICATION**
19 August 2020**PUBLISHED**
7 October 2020

Original content from this work may be used under the terms of the Creative Commons Attribution 4.0 licence.

Any further distribution of this work must maintain attribution to the author(s) and the title of the work, journal citation and DOI.



Environmental Research Letters

LETTER

Extreme event impacts on CO₂ fluxes across a range of high latitude, shrub-dominated ecosystems

Rachael Treharne¹ , Jarle W Bjerke² , Hans Tømmervik² and Gareth K Phoenix¹¹ Department of Animal and Plant Sciences, The University of Sheffield, Western Bank, Sheffield S10 2TN, United Kingdom² Norwegian Institute for Nature Research, High North Centre for Climate and the Environment, Tromsø NO-9296, NorwayE-mail: rachael.treharne@gmail.com**Keywords:** Arctic, Arctic browning, climate change, dwarf shrub, extreme events, snow cover, winterSupplementary material for this article is available [online](#)**Abstract**

The Arctic is experiencing an increased frequency of extreme events which can cause landscape-scale vegetation damage. Extreme event-driven damage is an important driver of the decline in vegetation productivity (termed ‘Arctic browning’) which has become an increasingly important component of pan-Arctic vegetation change in recent years. A limited number of studies have demonstrated that event-driven damage can have major impacts on ecosystem CO₂ balance, reducing ecosystem carbon sink strength. However, although there are many different extreme events that cause Arctic browning and different ecosystem types that are affected, there is no understanding of how impacts on CO₂ fluxes might vary between these, or of whether commonalities in response exist that would simplify incorporation of extreme event-driven Arctic browning into models.

To address this, the impacts of different extreme events (frost-drought, extreme winter warming, ground icing and a herbivore insect outbreak) on growing season CO₂ fluxes of Net Ecosystem Exchange (NEE), Gross Primary Productivity (GPP) and ecosystem respiration (R_{eco}) were assessed at five sites from the boreal to High Arctic (64°N–79°N) in mainland Norway and Svalbard. Event-driven browning had consistent, major impacts across contrasting sites and event drivers, causing site-level reductions of up to 81% of NEE, 51% of GPP and 37% of R_{eco}. Furthermore, at sites where plot-level NDVI (greenness) data were obtained, strong linear relationships between NDVI and NEE were identified, indicating clear potential for impacts of browning on CO₂ balance to be consistently, predictably related to loss of greenness across contrasting types of events and heathland ecosystems.

This represents the first attempt to compare the consequences of browning driven by different extreme events on ecosystem CO₂ balance, and provides an important step towards a better understanding of how ecosystem CO₂ balance will respond to continuing climate change at high latitudes.

1. Introduction

Rapidly rising temperatures in Arctic regions are causing extreme events to occur more frequently (Jentsch *et al* 2007, Bokhorst *et al* 2009, Vikhamar-Schuler *et al* 2016). These can cause vegetation damage and mortality at landscape or even regional scales, as has been observed through plot-level, regional and remote sensing studies (Beniston *et al* 2011; Bhatt *et al* 2013, Bjerke *et al* 2014, 2017, Treharne *et al* 2020). Extreme events are therefore

recognised as one of the key drivers of declining biomass and productivity at high latitudes, termed ‘Arctic browning’, which has become an increasingly important process in Arctic regions in recent years (Epstein *et al* 2015, 2016, Phoenix and Bjerke 2016), adding complexity to the previous decades of greening trends (Myers-Smith *et al* 2020).

Extreme event drivers of Arctic browning may be climatic, biological (e.g. defoliating insect outbreaks) or physical (e.g. fire) (Mack *et al* 2011, Jepsen *et al* 2013, Phoenix and Bjerke 2016). In the European

Arctic, the most damaging climatic events are extreme winter warming, frost drought and ice encapsulation. Extreme winter warming events involve abrupt temperature increases of as much as 25 °C in 24 h, causing rapid snowmelt and premature loss of freeze tolerance in exposed vegetation. A return to sub-zero winter temperatures then results in freezing damage (Bokhorst *et al* 2008, 2009, 2010). Frost drought occurs when vegetation adapted to a stable, insulating snow cover becomes exposed during winter due to low snow cover, from low snow fall, melt or high winds. The resulting transpiration by exposed plant shoots while the roots remain in frozen soil leads to desiccation and mortality (Tranquillini 1982, Bjerke *et al* 2017, Trehearne *et al* 2019). Ice encapsulation of plants through snow thaw-freeze and rain-on-snow events can cause severe damage to vegetation through a combination of hypoxia, CO₂ accumulation and exposure to greater temperature variability (Hansen *et al* 2014, Milner *et al* 2016), though some species may be generally tolerant (Preece *et al* 2012, Preece and Phoenix 2013, 2014). Changes in winter conditions are also altering the frequency and severity of biological events, for instance by increasing population outbreaks of defoliating insects, such as the caterpillars of the geometrid moths *Epirrita autumnata* and *Operophtera brumata* (Callaghan *et al* 2010, Jepsen *et al* 2013). Higher winter temperatures improve over-wintering egg survival and facilitate range expansion, increasing the incidence, intensity and duration of outbreaks (Wolf *et al* 2008, Johansson *et al* 2011).

The damage following such events can be considerable. In 2012 a combination of events caused Normalised Difference Vegetation Index (NDVI, a measure of greenness, and a proxy for biomass production) across the Nordic Arctic Region (NAR) to decline to the lowest values ever recorded (Bjerke *et al* 2014), while a single event in 2007 caused an NDVI reduction of more than 25% over >1400 km² (Bokhorst *et al* 2009). Such examples, while best documented in relatively southern regions of the Arctic, have been reported from sub-Arctic to High Arctic latitudes, and are expected to become increasingly important as the Arctic continues to undergo rapid climate change (Callaghan *et al* 2010, Hansen *et al* 2014, Graham *et al* 2017).

However, despite the observed scale of event-driven browning, the consequences for CO₂ balance of climatic and biological extreme events are not well understood. This is in contrast to a better understanding of the carbon balance impacts of other extreme event types; notably tundra fire and abrupt permafrost thaw (Mack *et al* 2011, Rocha and Shaver 2011, Jiang *et al* 2015, Cassidy *et al* 2016, 2017, Turetsky *et al* 2020). Insect outbreak studies show that browning linked to defoliation can be decisive in determining ecosystem carbon sink strength (Kurz *et al* 2008, Heliasz *et al* 2011, Parker *et al* 2017), and recent work

suggests that climatic extreme events such as frost-drought and extreme winter warming also have substantial impacts on CO₂ fluxes (Bokhorst *et al* 2011, Parmentier *et al* 2018, Trehearne *et al* 2019). However these studies remain rare; just one comprehensive, full-growing season assessment has been made of the impacts of climatic extreme event-driven browning on GPP, NEE and R_{eco}, finding that both GPP and NEE in sub-Arctic heathland were reduced by almost half by combined frost-drought and extreme winter warming impacts (Trehearne *et al* 2019). One further study has assessed how browning driven by an extreme climatic event in a northern peatland affected eddy covariance CO₂ fluxes (Parmentier *et al* 2018). This work was challenged by large inter-annual variability in summer climate, but nonetheless indicated a 12% reduction in GPP, further highlighting that browning has the potential to substantially impact CO₂ balance through shoot mortality and loss of photosynthetic area. However, understanding extreme event browning impacts on CO₂ fluxes remains challenging due to the diversity of event types that cause browning and the range of different vegetation that can be impacted.

There is therefore a need to develop a more robust understanding of event-driven browning impacts on ecosystem CO₂ balance, considering in particular whether ecosystem CO₂ flux impacts are (a) clearly and predictably related to damage severity and (b) comparable across different extreme event drivers and vegetation. In undamaged vegetation of high latitude ecosystems, linear relationships have been reported between Leaf Area Index (LAI) as predicted from NDVI, and GPP and NEE across multiple vegetation, allowing considerable simplification in quantifying ecosystem productivity across the Arctic (Street *et al* 2007, Shaver *et al* 2007). However, it is not clear whether these relationships will be maintained in vegetation exposed to extreme events, as evidence suggests that in some cases negative physiological effects following an event can impact ecosystem CO₂ fluxes without a clear, corresponding change in vegetation greenness (Bokhorst *et al* 2008, Trehearne *et al* 2019). Identifying such emergent relationships that work across different extreme event drivers and vegetation (where these relationships exist) is an important step towards determining the implications of Arctic browning for CO₂ balance at regional or greater scales (Beniston *et al* 2007, Graham *et al* 2017).

To address these issues, we assessed the impacts of extreme event-driven browning on growing season CO₂ fluxes in widespread, yet contrasting, heathland vegetation types affected by different browning drivers. Five sites along a 1600 km latitudinal gradient, spanning 15° of latitude, allowed us to capture emergent variation and commonalities in response in boreal, sub-Arctic and High Arctic regions, covering extreme winter warming, frost-drought, ground icing and insect outbreak as the drivers of damage.

Table 1. Summary of sites.

Name of site	Latitude ($^{\circ}$ N)	Ecosystem type	Dominant heathland species	Browning driver	Years of damage
Flatanger_B_WW	64.4	Boreal	<i>Calluna vulgaris</i>	Primary: extreme winter warming. Secondary: frost drought	Winter 2013–2014
Storfjord_S_FD	69.3	Sub-Arctic	<i>Empetrum nigrum</i>	Frost drought	Winter 2011–2012
Håkøya_S_IO	69.7	Sub-Arctic	<i>Empetrum nigrum</i>	Insect outbreak	Summer 2014, 2015
Longyearbyen_H_IE	78.2	High Arctic	<i>Cassiope tetragona</i>	Ice encapsulation	Winter 2012, 2015
Ny-Ålesund_H_IE	78.9	High Arctic	<i>Cassiope tetragona</i>	Ice encapsulation	Winter 2012, 2015

Plot-level measurements of NEE, GPP and R_{eco} were completed at each site at peak biomass across a range of undamaged to maximally damaged (heavily browned, most shoots dead) plots, while transects were used to survey site-level damage severity and scale up plot-level CO₂ fluxes across each site. In addition, plot-level NDVI was recorded at a sub-set of sites to assess whether clear relationships between NDVI and ecosystem CO₂ fluxes exist in browned vegetation.

We hypothesised that (i) browning would cause significant reductions in GPP and NEE across all sites; (ii) R_{eco} would decrease due to less carbon available for respiration from lower GPP (though increased leaf and root litter inputs from recently dead plants, in contrast, might stimulate microbial activity); (iii) site-level reduction in GPP and NEE would decrease with increasing latitude due to lower leaf area and productivity of healthy vegetation; (iv) where measured, clear linear relationships between CO₂ uptake (GPP and NEE) and NDVI would be identifiable when incorporating damaged and undamaged vegetation.

2. Methods

2.1. Study sites

Sites were located in the Norwegian boreal, sub-Arctic and High Arctic regions (covering latitudes from 64°N to 79°N) in areas known to have experienced extreme events in the preceding three years (table 1). Initials following site names denote region and primary driver of damage (e.g. ‘B_WW’ = boreal, extreme winter warming). Full descriptions of each site, and of the extreme event drivers which resulted in browning, can be found in the supporting information (section S1). At all sites, browning was clearly visible as dead, pale brown or grey shoots (figure S1 (<https://stacks.iop.org/ERL/15/104084/mmedia>)).

2.2. Ecosystem CO₂ flux measurements (NEE, GPP and R_{eco})

At each site flux measurements were taken on 12–22 plots. Plots were located to ensure the full range of browning severity present at the site was sampled. Measurements were completed in 2015 between 3

June and 17 June at Flatanger (17 plots), 21 June and 5 July on Svalbard (12 and 15 plots at Longyearbyen and Ny-Ålesund respectively) and between 8 July and 30 July at Storfjord_S_FD and Håkøya_S_IO (21 and 22 plots). While all measurements were therefore completed close to peak biomass, logistical constraints on the timing of measurements dictated that this sampling design may not have captured peak LAI at each site. LAI may have continued to increase after our measurements (e.g. Street *et al* 2007), but taking later measurements would not have been ideal due to environmental constraints on photosynthesis and the greater chance later-season of not having full sunny days to conduct light response curves.

NEE was measured using a LiCor LI6400 portable photosynthesis system (LiCor, Germany) and a custom 50 × 50 × 25 cm transparent acrylic vegetation chamber, with fans mixing the chamber air (following Williams *et al* 2006, Street *et al* 2007). At sites on Svalbard, a 20 × 20 × 20 cm chamber was used due to smaller vegetation stature and transport limitations. The chamber was placed on a rigid frame supported by aluminium poles driven into the ground. A seal was provided between the chamber and frame by a rubber gasket, and between the frame and ground surface by a flexible, transparent plastic skirt weighted down with steel chains. Photosynthetically active radiation (PAR) was recorded using a LiCor Quantum sensor mounted inside the vegetation chamber. Enclosed volume was determined by using measurements of the height of the frame from the ground across a grid of nine points to calculate volume as four hexahedrons in addition to the chamber volume (which sat on top of this frame volume). Within the chamber, CO₂ concentration was measured every 2 s for 50 s. Where PAR varied by >15%, measurements were discarded at the analysis stage. Measurements were carried out at five light levels (full light, three successive levels of shading and dark) in a randomised order using optically neutral shade cloths and tarpaulin to cover the chamber. The chamber was allowed to return to ambient CO₂ between measurements.

Light response curves of NEE and GPP were calculated following Treharne *et al* (2019). In brief, CO₂

concentration over time was converted to CO₂ flux, allowing the light response of net ecosystem exchange to be modelled as a rectangular hyperbola with a term for ecosystem respiration (R_{eco}). This modelled term was used for R_{eco}. Subtraction of R_{eco} from CO₂ flux measurements enabled a light response curve of GPP to be fitted, and thus GPP to be standardised at a PAR of 600 μmol s PPF m⁻² s⁻¹ (GPP₆₀₀). GPP₆₀₀ represents flux at a medium light level and has been used previously to compare GPP between vegetation plots in the field (Street *et al* 2007, Trehearne *et al* 2019). NEE was also standardised at this light level (NEE₆₀₀). Other approaches can be used to interpret chamber flux data, such as modelling that includes parametrisation and calibration for individual vegetation types (Williams *et al* 2006) or that work for a diversity of vegetation (e.g. Shaver *et al* 2007); these can have advantages for understanding fluxes from different vegetation types under different conditions. Our approach was used since our primary aim was to compare fluxes at an intermediate light level under the environmental conditions at the time of measurement, and therefore does not account for (or model) variation that is caused by e.g. temperature and soil moisture.

2.3. Visual estimates of browning and NDVI

Percentage cover of dead shoots ('percentage browned'), was visually estimated at each plot using a quadrat matched to the size of the plot along with percentage cover of dominant species and percentage of dominant species cover that was browned (termed 'damage intensity'). Site-level browning was assessed through simple transect surveys of percentage cover of dominant species and of browned vegetation using a 50 × 50 cm quadrat (supporting information, section S2).

Reflectance data were recorded at each plot in two sites: Flatanger_B_WW and Håkøya_S_IO. This was done using a standard DSLR camera (Canon 450D) in which the usual light sensor was replaced with an infrared sensor by optics company Llewellyn Data Processing (MaxMax.com, New Jersey), enabling the camera to record visible light in the blue channel and near infrared in the red channel (Llewellyn Data Processing, New Jersey). This camera was calibrated by using a white square to manually set white balance prior to taking measurements at each site. NDVI was calculated from reflectance data photos using ENVI 5.2 (Exelis Visual Information Solutions, Boulder, Colorado).

2.4. Statistical analysis

Linear regression was used to identify relationships between CO₂ fluxes and vegetation damage at each site. Linear regression parameters were then used to estimate the site level reductions in CO₂ fluxes at the mean level of damage across each site compared to undamaged vegetation. At Ny-Ålesund, non-linear

regressions were also fitted using self-starting asymptotic models, due to visually apparent non-linearity in the plotted data. The goodness of fit provided by linear and non-linear models at Ny-Ålesund was assessed by using an F-test (analysis of variance) to compare residual sum of squares, and by comparing AIC values. All statistical analyses were carried out in R (R Core Team, 2017).

3. Results

3.1. Impacts of browning on NEE, GPP and R_{eco}

3.1.1. Impacts of browning on C fluxes

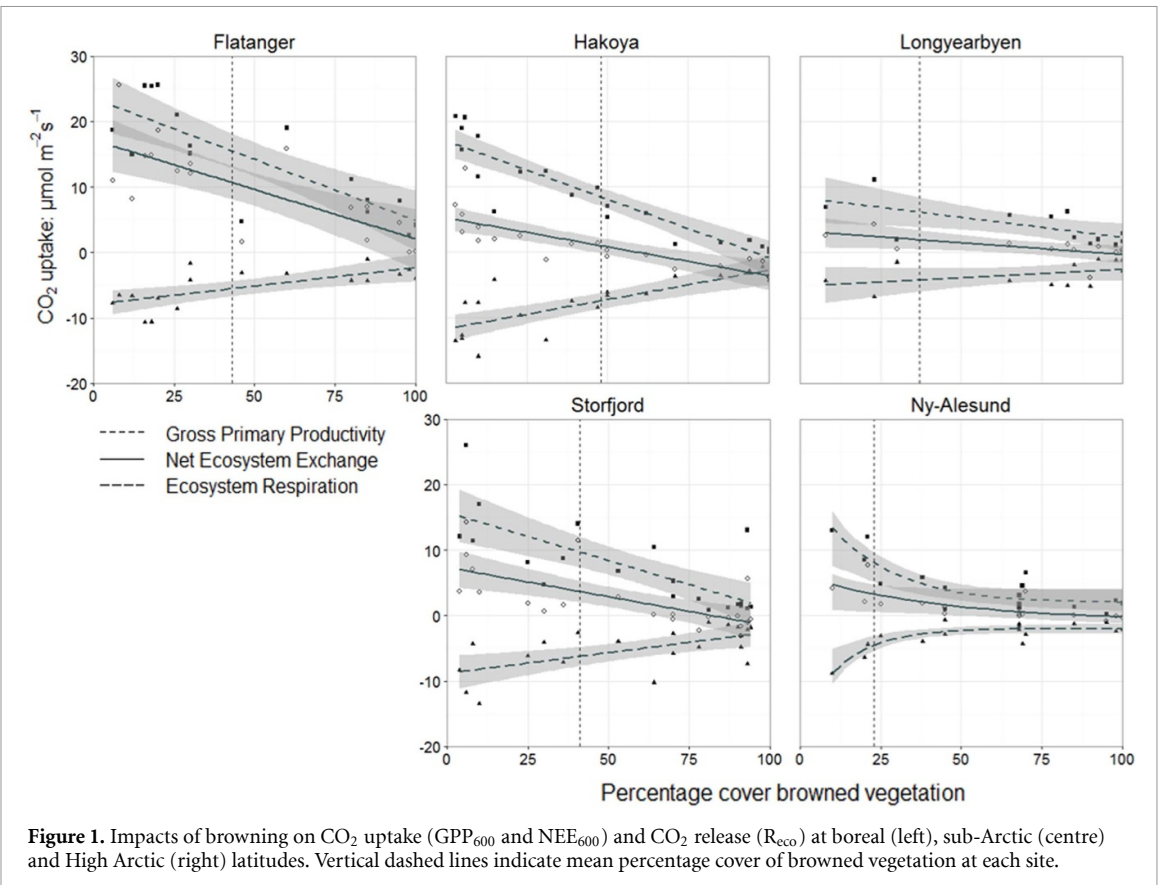
Significant linear declines in both GPP₆₀₀ and NEE₆₀₀ with increasing percentage browned were identified at all sites (figure 1, table 2 for statistics). These relationships explained up to 82% and 61% of variation in GPP₆₀₀ and NEE₆₀₀ respectively (at Håkøya_S_IO).

The negative correlations between percent browned and GPP₆₀₀ and NEE₆₀₀ were steepest at Flatanger_B_WW, where percent browned explained 65% and 53% of variation in each flux respectively. The slopes of these relationships were shallowest at Longyearbyen_H_IE while nonetheless explaining 37% and 32% of variation in GPP₆₀₀ and NEE₆₀₀ respectively.

R_{eco} also decreased with percent browned at all sites except Longyearbyen_H_IE. The negative relationships between R_{eco} and percent browned explained between 37% and 59% of variation in this flux (at Storfjord_S_FD and H Håkøya_S_IO respectively), and were steepest at these sub-Arctic sites, where R_{eco} in undamaged vegetation was higher than at boreal or High Arctic sites.

At the High Arctic site Ny-Ålesund_H_IE, linear regressions of all three CO₂ fluxes and percent browned were significant. However, an asymptotic regression model provided a better fit for GPP₆₀₀ (Reduction in RSS = 33.9, F = 7.86, p = 0.015) and for R_{eco} (Reduction in RSS = 19.67, F = 16.37, p = 0.001), but was not significantly different to a linear regression in the case of NEE₆₀₀. Nonetheless, linear regressions were used to estimate site-level impacts (see below) at Ny-Ålesund_H_IE. This was partly to maximise comparability of estimates between sites, and partly due to concern that the accuracy of the nonlinear regressions fitted may be limited, particularly at low values of percent browned, by a relative lack of plots with very little damage assessed at Ny-Ålesund_H_IE, compared to other sites.

When data from all sites were combined, linear declines in all measured fluxes with increasing percent browned remain significant (figure S3; GPP₆₀₀: R² = 0.55, p < 0.001, NEE₆₀₀: R² = 0.332, p < 0.001, R_{eco}: R² = 0.413, p < 0.001). Multiple regressions of GPP₆₀₀, NEE₆₀₀ and R_{eco} against percent browned and dominant heathland species (*Calluna vulgaris*, *Empetrum nigrum* or *Cassiope tetragona*) explain 69%



of overall variation in GPP_{600} , 63% in NEE_{600} and 50% in R_{eco} ($p < 0.001$).

3.1.2. Site level browning and estimated changes in C fluxes

Substantial and somewhat similar levels of damage were recorded at all sites. Mean percentage cover of damaged vegetation (percent browned) ranged from 23% to 48%, with damage intensity (the proportion of the dominant species showing damage) ranging from 56% to 80% (table 3, figure S2).

Site-level reductions in CO_2 uptake were largest in absolute terms at Flatanger_B_WW (figure 2). While reductions were lower at the sub-Arctic insect outbreak and frost-drought sites Håkøya_S_IO and Storfjord_S_FD, lower baseline productivity in the sub-Arctic region meant that these reductions accounted for the largest proportion of the productivity of healthy vegetation, with GPP_{600} reduced by 51% and 41% and NEE_{600} by 81% and 61% at Håkøya_S_IO and Storfjord_S_FD respectively.

Site-level reductions in CO_2 uptake were lowest at High Arctic ice encapsulation sites, where GPP_{600} was reduced by 23%–27%. The smaller reductions here were partly due to lower mean percent browned values at High Arctic sites; at a percent browned of 50%, GPP_{600} reductions at Longyearbyen_H_IE and Ny-Ålesund_H_IE were 36% and 49% respectively,

comparable with values of between 41% and 53% at the other sites at the same level of browning.

3.2. Relationships between NDVI and fluxes

Strong linear relationships were identified between GPP_{600} and NDVI, with NDVI explaining 78% of variation in GPP_{600} at the boreal extreme winter warming site Flatanger_B_WW and 91% at the sub-Arctic insect outbreak site Håkøya_S_IO (figure 3(a); Flatanger_B_WW: $R^2 = 0.783$, fitted line: $y = 3.537 + 30.158x$, $DF = 1, 15$, $p < 0.001$, Håkøya_S_IO: $R^2 = 0.913$, fitted line: $y = -13.381 + 43.801x$, $DF = 1, 14$, $p < 0.001$). A significant relationship explaining 49% of variation in GPP_{600} was maintained when data from both sites were combined ($R^2 = 0.492$, fitted line: $y = -0.2321 + 27.707x$, $DF = 1, 31$, $p < 0.001$). Significant relationships between NDVI and NEE_{600} also explained 67% and 80% of NEE_{600} at Flatanger_B_WW and Håkøya_S_IO respectively (figure 3(b); Flatanger_B_WW: $R^2 = 0.671$, fitted line: $y = 1.252 + 22.456x$, $DF = 1, 31$, $p < 0.001$, Håkøya_S_IO: $R^2 = 0.796$, fitted line: $y = -10.775 + 23.844x$, $DF = 1, 14$, $p < 0.001$). A significant relationship was maintained when data from both sites were combined, albeit with lower explanatory power ($R^2 = 0.223$). Relationships between NDVI and fluxes are further supported by the strong linear

Table 2. Coefficients and summary statistics for linear regressions of percentage cover of damaged vegetation against GPP₆₀₀, NEE₆₀₀ and ecosystem respiration at each site.

Site	Gross primary productivity					Net ecosystem exchange					Ecosystem respiration			
	Slope	Intercept	R ²	p value	RSE	Slope	Intercept	R ²	p value	RSE	Slope	Intercept	R ²	p value
Flatanger_B_WW	-0.21	25.10	0.65	<0.001	5.25	-0.15	17.20	0.53	<0.001	4.86	0.06	-7.94	0.42	<0.01
Storfjord_S_FD	-0.18	18.20	0.55	<0.001	5.50	-0.09	7.38	0.43	<0.001	3.44	0.09	-10.80	0.37	<0.01
Håkoya_S_IO	-0.18	17.00	0.82	<0.001	3.03	-0.09	5.24	0.61	<0.001	2.51	0.09	-11.80	0.59	<0.001
Longyearbyen_H_IE	-0.06	8.40	0.37	0.02	2.42	-0.04	3.25	0.32	0.03	1.54	0.03	-5.16	0.09	0.18
Ny-Alesund_H_IE	-0.10	10.40	0.57	<0.001	2.53	-0.05	4.38	0.44	<0.001	1.64	0.05	-6.00	0.45	<0.01
														1.59

Table 3. Mean degree of damage assessed visually across transects at each site, presented as both overall mean percentage cover of damage and mean percentage of the dominant species showing damage. Standard error is shown in brackets.

	Site				
	Flatanger_B_WW	Storfjord_S_FD	Håkøya_S_IO	Longyearbyen_H_IE	Ny-Ålesund_H_IE
Mean percentage cover of damaged vegetation	43 (2.00)	42 (4.48)	48 (2.43)	37 (2.80)	23 (3.27)
Mean damage intensity (percentage of dominant species showing damage)	66 (2.48)	51 (4.41)	76 (2.61)	80 (2.31)	56 (3.96)
Total number of 1 square metre plots surveyed	30	28	12	20	16

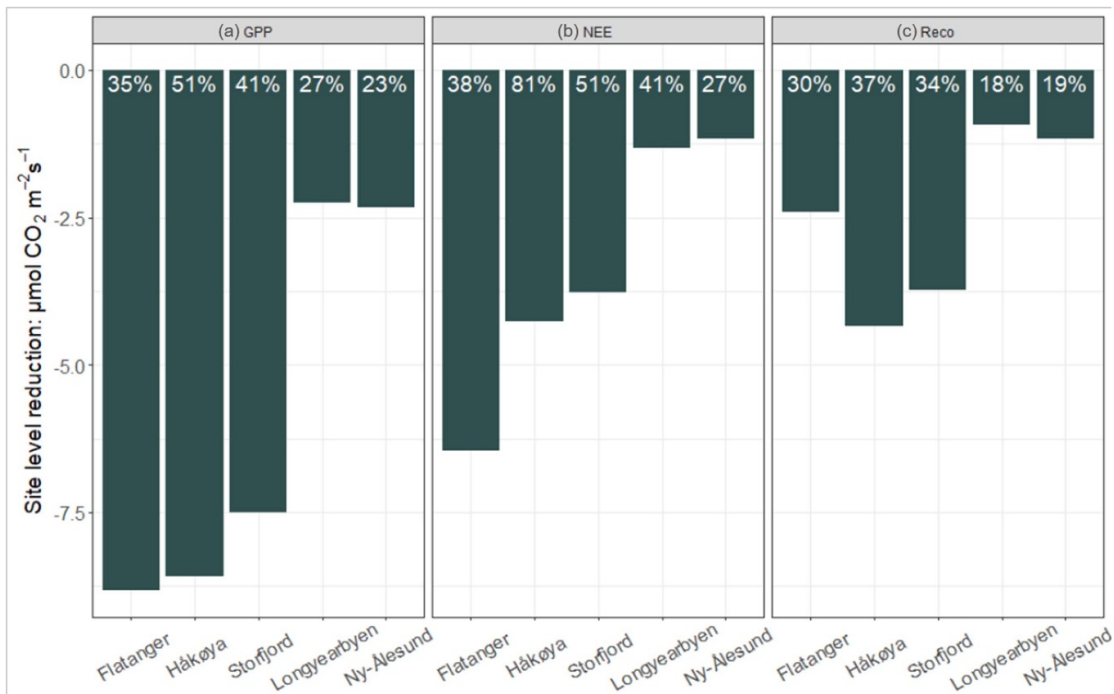


Figure 2. Reduction in (a) GPP₆₀₀ (b) NEE₆₀₀ and (c) ecosystem respiration at the mean percentage cover of browned vegetation for each site, arranged from boreal to High Arctic sites running left to right. Bar labels indicate the percentage of each flux in healthy vegetation at the same site that this reduction represents.

relationship between percentage cover browned and NDVI (figure S4).

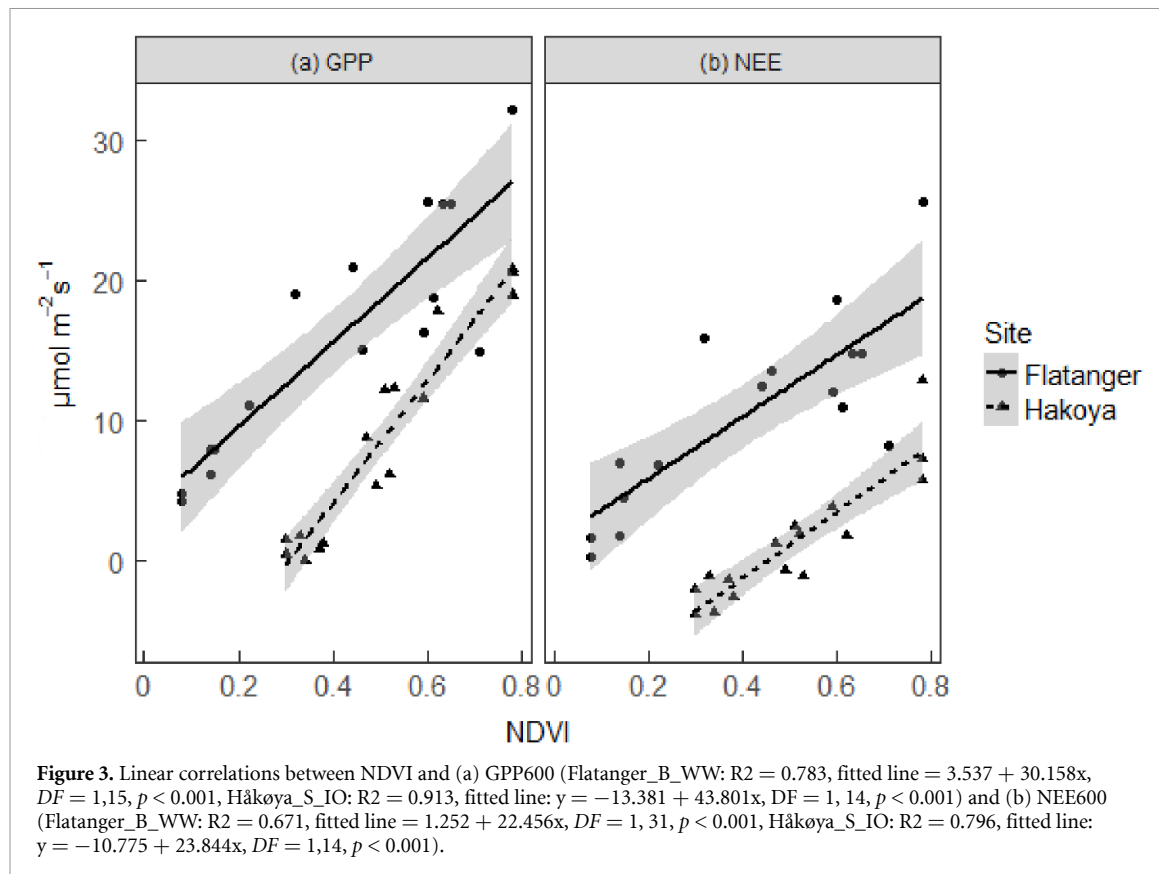
4. Discussion

This first detailed assessment of the consequences for ecosystem CO₂ fluxes of browning resulting from a range of different extreme event drivers has shown major impacts on GPP₆₀₀, R_{eco} and NEE₆₀₀, representing a substantial reduction in carbon sequestration capacity at peak biomass when productivity should be at its highest. Impacts are comparable across all event drivers, and their magnitudes are clearly and predictably linked to the severity of damage, as measured both by visual observation (percent browned) and plot-level NDVI (recorded at two

sites). These consistent, linear relationships do not explicitly take into account factors which are likely to differ between vegetation types, such as the contribution to CO₂ fluxes of non-vascular species which may be less severely impacted compared to vascular species (Bjerke *et al* 2011). Nonetheless, identification of emergent relationships with NDVI across heathland sites indicates potential to assess extreme event impacts on peak season CO₂ fluxes using proximally or remotely sensed NDVI.

4.1. Impact of damage on GPP and NEE

Reductions in both GPP₆₀₀ and NEE₆₀₀ were clearly and consistently related to the severity of damage across the full range of sites, indicating a high commonality in the response of CO₂ uptake to



browning caused by different extreme event drivers. This consistency was particularly marked between Håkøya_S_IO and Storfjord_S_FD in the sub-Arctic, where the regression slopes of NEE₆₀₀ and GPP₆₀₀ with percent browned were very similar, despite the very different drivers and timing of damage at these two sites (defoliating insect outbreak, 2014–2015, and frost-drought, 2011–2012). Inter-site differences in the relationship between CO₂ uptake and browning severity (steeper slopes at more southerly sites) that were present were primarily driven by differences in productivity in contrasting heathland types. Browning severity and corresponding GPP₆₀₀ reductions were still high and comparable with more recently damaged sites at Storfjord_S_FD, even following three growing seasons of recovery. This suggests a caveat to previous work reporting quick recovery from event-driven browning (Bokhorst *et al* 2012): where damage is severe and results in extensive mortality, recovery may be slower, allowing landscape-level consequences for CO₂ uptake to persist over several years.

However, while there was a significant linear GPP₆₀₀–percent browned relationship at Ny-Ålesund_H IE, a nonlinear model provided a better fit to the data at this site. This nonlinear relationship reflects larger reductions in CO₂ uptake at lower levels of percent browned compared with other sites, indicating that extreme event exposure may have negatively impacted surviving, green vegetation.

Previous studies have shown that ice encapsulation can have physiological impacts on undamaged shoots, including reducing flowering and berry production in some Arctic species (Preece *et al* 2012, Preece and Phoenix 2013, Milner *et al* 2016). This nonlinearity between GPP₆₀₀ and percent browned may indicate that physiological damage extends to photosynthetic capacity, reducing CO₂ uptake beyond what would be expected based on observed shoot mortality. This may be linked to the ‘stress response’ observed in surviving vegetation following exposure to other extreme climatic events, visible as deep red pigmentation (Trehearne *et al* 2019).

Upscaling browning impacts on GPP₆₀₀ and NEE₆₀₀ to the site-level using damage surveys indicates major overall reductions in productivity, similar to or greater than those identified by initial assessments of climatic extreme events in similar regions (Bokhorst *et al* 2011, Parmentier *et al* 2018). These reductions were largest in absolute terms at boreal latitudes, where productivity of undamaged vegetation is highest, but largest as a proportion of baseline productivity at sub-Arctic sites, where heavily damaged vegetation plots were even converted to a net CO₂ source. Although site-level effects of damage in the High Arctic, where GPP₆₀₀ was reduced by 23–27%, were smaller than at other latitudes, these impacts remain important as the brevity of the growing season means productivity at peak biomass is particularly crucial in the High Arctic (Larsen *et al* 2007). Even

a relatively small reduction in peak biomass GPP₆₀₀ may therefore substantially alter annual CO₂ balance.

4.2. Impact of damage on ecosystem respiration

As predicted, R_{eco} decreased at all sites with increasing percent browned (although this was not statistically significant at Longyearbyen_H_IE). Stable or reduced R_{eco} following insect outbreak and frost events has previously been attributed to reduced leaf respiration and root growth, reduced microbial abundance and activity, and microbial mortality, resulting from decreased carbon transfer belowground (Grogan *et al* 2004, Read *et al* 2004, Christiansen *et al* 2012, Zhao *et al* 2017, Olsson *et al* 2017, Parker *et al* 2017). Parker *et al* (2017) argue that where increased respiration is observed following insect outbreak (e.g. Frost and Hunter 2004), this reflects increased belowground carbon allocation in an attempt to recover lost nitrogen, and is a response to comparatively mild defoliation damage. In contrast, Parker *et al* (2017) also show that after total defoliation, belowground carbon allocation decreases, slowing soil processes including respiration. The results presented here support this, further suggesting that climatic extreme events can result in a similar deceleration of soil processes, as has previously been indicated by observations of reduced root and mycorrhizal biomass following an extreme winter warming field simulation (Bokhorst *et al* 2009).

4.3. Relationships between NDVI and CO₂ fluxes

Strong linear relationships between NDVI and both GPP₆₀₀ and NEE₆₀₀ were identified at sites where NDVI was measured ($R^2 = 0.67\text{--}0.91$). These were maintained when data from both sites were combined, although in the case of NEE₆₀₀ the explanatory power of this relationship was low ($R^2 = 0.22$). This suggests that with a simple characterisation of widespread Arctic heathland (e.g. dominant species), change in NDVI can provide a direct, accurate estimate of CO₂ uptake reduction following extreme event-driven browning. None-the-less, even without knowing the identity of the dominant species, an acceptable estimate of GPP reduction in heathland may be made.

Previous work has found an exponential relationship between NDVI and GPP₆₀₀, explaining 75% of variation in GPP₆₀₀ across multiple Arctic vegetation types (Street *et al* 2007). That a linear, rather than an exponential, relationship is seen in our work may be linked to consistency in canopy structure and in photosynthetic activity of healthy vegetation within the heathland communities considered here (Steltzer and Welker 2006). Arctic heathland has a relatively homogenous canopy structure, meaning increases in greenness reflect proportional increases in leaf area. In contrast, when a broader range of Arctic vegetation types is considered, an increase in NDVI from a low value may correspond to a smaller increase in LAI

compared to the same NDVI increase at higher values. For example, an NDVI increase from a low value may reflect increasing total vegetation cover, while an NDVI increase from a high value is likely to reflect a greater increase in LAI in a plant community where the canopy is already closed. As LAI drives GPP, this means a linear NDVI—GPP₆₀₀ relationship within a distinct vegetation type with a homogenous canopy structure is consistent with an exponential, pan-Arctic relationship across multiple vegetation types and canopy structures.

5. Conclusions

Extreme event-driven Arctic browning caused major reductions in key ecosystem CO₂ fluxes from boreal to High Arctic latitudes. Relationships between CO₂ fluxes and the extent of visible damage were consistent, demonstrating that net impacts are overwhelmingly determined by the severity of damage, regardless of the cause of browning. Furthermore, clear linear relationships between CO₂ uptake and NDVI highlight potential to use proximally or remotely sensed vegetation indices to assess damage impacts on CO₂ fluxes in widespread Arctic dwarf shrub heathland. Given the considerable consequences outlined here of event-driven browning for landscape CO₂ balance, and predictions for increasing frequency of extreme events as part of climate change there is a clear need to build on this work to upscale the impacts of extreme event-driven browning across Arctic regions, and incorporate these impacts into predictions of vegetation change and estimations of carbon balance in the Arctic.

Acknowledgments

RT was supported by the Adapting to the Challenges of a Changing Environment (ACCE) doctoral training partnership, funded by the Natural Environment Research Council (grant award NE/L002450/1). JWB and HT received financial support from the Polish–Norwegian Programme of the EEA Norway Grants (project 198571) and by FRAM–High North Research Centre for Climate and the Environment through its terrestrial flagship program (project 362222). We are grateful to the Norwegian Institute for Nature Research (NINA) for logistical support and to Laura Stendardi (Free University of Bozen Bolzano, Italy) for help in the field.

Data availability statement

The data that support the findings of this study are available upon reasonable request from the authors.

ORCID iDs

- Rachael Trehearne  <https://orcid.org/0000-0002-3238-5959>
 Hans Tømmervik  <https://orcid.org/0000-0001-7273-1695>

References

- Beniston M *et al* 2007 Future extreme events in European climate: an exploration of regional climate model projections *Clim. Change* **81** 71–95
- Bhatt U S, Walker D A, Raynolds M K, Bieniaek P A, Epstein H E, Comiso J C, Pinzon J E, Tucker C J and Polyakov I V 2013 Recent declines in warming and vegetation greening trends over Pan-Arctic Tundra *Remote Sens.* **5** 4229–54
- Bjerke J W, Bokhorst S, Zielke M, Callaghan T V, Bowles F W and Phoenix G K 2011 Contrasting sensitivity to extreme winter warming events of dominant sub-Arctic heathland bryophyte and lichen species *Nature* **99** 1481–88
- Bjerke J W, Karlsen S R, Høgda K A, Malnes E, Jepsen J U, Lovibond S, Vikhamar-Schuler D and Tømmervik H 2014 Record-low primary productivity and high plant damage in the Nordic Arctic region in 2012 caused by multiple weather events and pest outbreaks *Environ. Res. Lett.* **9** 084006
- Bjerke J W, Trehearne R, Vikhamar-Schuler D, Karlsen S R, Ravalainen V, Bokhorst S, Phoenix G K, Bochenek Z and Tømmervik H 2017 Understanding the drivers of extensive plant damage in boreal and Arctic ecosystems: insights from field surveys in the aftermath of damage *Sci. Total Environ.* **599–600** 1965–76
- Bokhorst S F, Bjerke J W, Tømmervik H, Callaghan T V and Phoenix G K 2009 Winter warming events damage sub-Arctic vegetation: consistent evidence from an experimental manipulation and a natural event *J. Ecol.* **97** 1408–15
- Bokhorst S F, Tømmervik H, Callaghan T V, Phoenix G K and Bjerke J W 2012 Vegetation recovery following extreme winter warming events in the sub-Arctic estimated using NDVI from remote sensing and handheld passive proximal sensors *Environ. Exp. Bot.* **81** 18–25
- Bokhorst S, Bjerke J W, Bowles F W, Melillo J, Callaghan T V and Phoenix G K 2008 Impacts of extreme winter warming in the sub-Arctic: growing season responses of dwarf shrub heathland *Glob. Change Biol.* **14** 2603–2612
- Bokhorst S, Bjerke J W, Melillo J, Callaghan T V and Phoenix G K 2010 Impacts of extreme winter warming events on litter decomposition in a sub-Arctic heathland *Soil Biol. Biochem.* **42** 611–7
- Bokhorst S, Bjerke J W, Street L E, Callaghan T V and Phoenix G K 2011 Impacts of multiple extreme winter warming events on sub-Arctic heathland: phenology, reproduction, growth, and CO₂ flux responses: impacts of multiple extreme winter warming events *Glob. Change Biol.* **17** 2817–30
- Callaghan T V, Bergholm F, Christensen T R, Jonasson C, Kokfelt U and Johansson M 2010 A new climate era in the sub-Arctic: accelerating climate changes and multiple impacts *Geophys. Res. Lett.* **37** L14705
- Cassidy A E, Christen A and Henry G H R 2016 The effect of a permafrost disturbance on growing-season carbon-dioxide fluxes in a high Arctic tundra ecosystem *Biogeosciences* **13** 2291–303
- Cassidy A E, Christen A and Henry G H R 2017 Impacts of active retrogressive thaw slumps on vegetation, soil, and net ecosystem exchange of carbon dioxide in the Canadian High Arctic *Arct. Sci.* **3** 179–202
- Christiansen C T, Svendsen S H, Schmidt N M and Michelsen A 2012 High arctic heath soil respiration and biogeochemical dynamics during summer and autumn freeze-in – effects of long-term enhanced water and nutrient supply *Glob. Change Biol.* **18** 3224–36
- Epstein H E *et al* 2016 Tundra Greenness Arctic Report Card: Update for 2016 eds J E Overland and J T Mathis NOAA, Silver Spring, MD <http://www.arctic.noaa.gov/reportcard/>
- Epstein H E *et al* 2015 Tundra Greenness Arctic Report Card: Update for 2015 eds, J Richter-Menge and J E Overland NOAA, Silver Spring, MD <http://www.arctic.noaa.gov/reportcard/>
- Frost C J and Hunter M D 2004 Insect canopy herbivory and frass deposition affect soil nutrient dynamics and export in oak mesocosms *Ecology* **85** 3335–47
- Graham R M, Cohen L, Petty A A, Boisvert L N, Rinke A, Hudson S R, Nicolaus M and Granskog M A 2017 Increasing frequency and duration of Arctic winter warming events *Geophys. Res. Lett.* **44** 6974–83
- Grogan P, Michelsen A, Ambus P and Jonasson S 2004 Freeze–thaw regime effects on carbon and nitrogen dynamics in sub-arctic heath tundra mesocosms *Soil Biol. Biochem.* **36** 641–54
- Hansen B B, Isaksen K, Benestad R E, Kohler J, Pedersen Å Ø, Loe L E, Coulson S J, Larsen J O and Varpe Ø 2014 Warmer and wetter winters: characteristics and implications of an extreme weather event in the High Arctic *Environ. Res. Lett.* **9** 114021
- Heliasz M, Johansson T, Lindroth A, Mölder M, Mastepanov M, Friberg T, Callaghan T V and Christensen T R 2011 Quantification of C uptake in subarctic birch forest after setback by an extreme insect outbreak *Geophys. Res. Lett.* **38** L01704
- Jentsch A, Kreyling J and Beierkuhnlein C 2007 A new generation of climate-change experiments: events, not trends *Frontiers Ecol. Environ.* **5** 365–74
- Jepsen J U, Biuw M, Ims R A, Kapari L, Schott T, Windstad O P L and Hagen S B 2013 Ecosystem impacts of a range expanding forest defoliator at the Forest-Tundra Ecotone *Ecosystems* **16** 561–75
- Jiang Y, Rastetter E B, Rocha A V, Pearce A R, Kwiatkowski B L and Shaver G R 2015 Modeling carbon–nutrient interactions during the early recovery of tundra after fire *Ecol. Appl.* **25** 1640–52
- Johansson C, Pohjola V A, Jonasson C and Callaghan T V 2011 Multi-decadal changes in snow characteristics in Sub-Arctic Sweden *AMBIO* **40** 566–74
- Kurz W A, Dymond C C, Stinson G, Rampley G J, Neilson E T, Carroll A L, Ebata T and Safranyik L 2008 Mountain pine beetle and forest carbon feedback to climate change *Nature* **452** 987–90
- Larsen K S, Ibrom A, Jonasson S, Michelsen A and Beier C 2007 Significance of cold-season respiration and photosynthesis in a subarctic heath ecosystem in Northern Sweden *Glob. Change Biol.* **13** 1498–508
- Mack M C, Bret-Harte M S, Hollingsworth T N, Jandt R R, Schuur E A G, Shaver G R and Verbyla D L 2011 Carbon loss from an unprecedented Arctic tundra wildfire *Nature* **475** 489–92
- Milner J M, Varpe Ø, van der Wal R and Hansen B B 2016 Experimental icing affects growth, mortality, and flowering in a high Arctic dwarf shrub *Ecol. Evol.* **6** 2139–48
- Myers-Smith I H *et al* 2020 Complexity revealed in the greening of the Arctic *Nat. Clim. Change* **10** 106–17
- Olsson P-O, Heliasz M, Jin H and Eklundh L 2017 Mapping the reduction in gross primary productivity in subarctic birch forests due to insect outbreaks *Biogeosciences* **14** 1703–19
- Parker T C, Sadowsky J, Dunleavy H, Subke J-A, Frey S D and Wookey P A 2017 Slowed biogeochemical cycling in sub-arctic birch forest linked to reduced mycorrhizal growth and community change after a defoliation event *Ecosystems* **20** 316–30
- Parmentier F-J W, Rasse D P, Lund M, Bjerke J W, Drake B G, Weldon S, Tømmervik H and Hansen G H 2018 Vulnerability and resilience of the carbon exchange of a

- subarctic peatland to an extreme winter event *Environ. Res. Lett.* **13** 065009
- Phoenix G K and Bjerke J W 2016 Arctic browning: extreme events and trends reversing arctic greening *Glob. Change Biol.* **22** 2960–2
- Preece C, Callaghan T V and Phoenix G K 2012 Impacts of winter icing events on the growth, phenology and physiology of sub-arctic dwarf shrubs *Physiol. Plant.* **146** 460–72
- Preece C and Phoenix G K 2013 Responses of sub-arctic dwarf shrubs to low oxygen and high carbon dioxide conditions *Environ. Exp. Bot.* **85** 7–15
- Preece C and Phoenix G K 2014 Impact of early and late winter icing events on sub-arctic dwarf shrubs *Plant Biol.* **16** 125–32
- Read D J, Leake J R and Perez-Moreno J 2004 Mycorrhizal fungi as drivers of ecosystem processes in heathland and boreal forest biomes *Can. J. Bot.* **82** 1243–63
- Rocha A V and Shaver G R 2011 Burn severity influences postfire CO₂ exchange in arctic tundra *Ecol. Appl.* **21** 477–89
- Shaver G R, Street L E, Rastetter E B, Van Wijk M T and Williams M 2007 Functional convergence in regulation of net CO₂ flux in heterogeneous tundra landscapes in Alaska and Sweden *J. Ecol.* **95** 802–17
- Steltzer H and Welker J M 2006 Modeling the effect of photosynthetic vegetation properties on the Ndvi–Lai Relationship *Ecology* **87** 2765–72
- Street L E, Shaver G R, Williams M and Van Wijk M T 2007 What is the relationship between changes in canopy leaf area and changes in photosynthetic CO₂ flux in arctic ecosystems? *J. Ecol.* **95** 139–50
- Tranquillini W 1982 Frost-drought and its ecological significance *Physiological Plant Ecology II* (Berlin, Heidelberg: Springer) pp 379–400
- Treharne R, Bjerke J W, Tømmervik H and Phoenix G K 2020 Development of new metrics to assess and quantify climatic drivers of extreme event driven Arctic browning *Remote Sens. Environ.* **243** 111749
- Treharne R, Bjerke J W, Tømmervik H, Stendardi L and Phoenix G K 2019 Arctic browning: impacts of extreme climatic events on heathland ecosystem CO₂ fluxes *Glob. Change Biol.* **25** 489–503
- Turetsky M R et al 2020 Carbon release through abrupt permafrost thaw *Nat. Geosci.* **13** 138–43
- Vikhamar-Schuler D, Isaksen K, Haugen J E, Tømmervik H, Luks B, Schuler T V and Bjerke J W 2016 Changes in winter warming events in the Nordic Arctic Region *J. Clim.* **29** 6223–44
- Williams M, Street L E, van Wijk M T and Shaver G R 2006 Identifying differences in carbon exchange among Arctic ecosystem types *Ecosystems* **9** 288–304
- Wolf A, Kozlov M V and Callaghan T V 2008 Impact of non-outbreak insect damage on vegetation in northern Europe will be greater than expected during a changing climate *Clim. Change* **87** 91–106
- Zhao J, Peichl M and Nilsson M B 2017 Long-term enhanced winter soil frost alters growing season CO₂ fluxes through its impact on vegetation development in a boreal peatland *Glob. Change Biol.* **23** 3139–53